



Available online at www.sciencedirect.com

ScienceDirect



RESEARCH ARTICLE

Identification of QTL and underlying genes for root system architecture associated with nitrate nutrition in hexaploid wheat



CrossMark

Marcus GRIFFITHS¹, Jonathan A. ATKINSON^{2,3}, Laura-Jayne GARDINER⁴, Ranjan SWARUP¹, Michael P. POUND⁵, Michael H. WILSON^{2,3}, Malcolm J. BENNETT^{1,2,3}, Darren M. WELLS^{1,2,3}

¹ School of Biosciences, University of Nottingham, Sutton Bonington Campus, LE12 5RD, UK

² Future Food Beacon of Excellence, University of Nottingham, Sutton Bonington Campus, LE12 5RD, UK

³ Integrative Phenomics Group, School of Biosciences, University of Nottingham, Sutton Bonington Campus, LE12 5RD, UK

⁴ IBM Research, The Hartree Centre, Warrington, WA4 4AD, UK

⁵ School of Computer Science, University of Nottingham, Nottingham, NG8 1BB, UK

Abstract

The root system architecture (RSA) of a crop has a profound effect on the uptake of nutrients and consequently the potential yield. However, little is known about the genetic basis of RSA and resource adaptive responses in wheat (*Triticum aestivum* L.). Here, a high-throughput germination paper-based plant phenotyping system was used to identify seedling traits in a wheat doubled haploid mapping population, Savannah×Rialto. Significant genotypic and nitrate-N treatment variation was found across the population for seedling traits with distinct trait grouping for root size-related traits and root distribution-related traits. Quantitative trait locus (QTL) analysis identified a total of 59 seedling trait QTLs. Across two nitrate treatments, 27 root QTLs were specific to the nitrate treatment. Transcriptomic analyses for one of the QTLs on chromosome 2D, which was found under low nitrate conditions, revealed gene enrichment in N-related biological processes and 28 differentially expressed genes with possible involvement in a root angle response. Together, these findings provide genetic insight into root system architecture and plant adaptive responses to nitrate, as well as targets that could help improve N capture in wheat.

Keywords: doubled-haploid population, nitrate, RNA-seq, quantitative trait loci, root system architecture, *Triticum aestivum* L. (wheat)

1. Introduction

Nitrogen (N) is an essential macronutrient for plant growth and development, and agriculture is heavily dependent on synthetic N fertilisers for enhancing productivity. Global demand for fertilisers is projected to rise by 1.5% each year, reaching 201 million tonnes in 2022, over half of which (112 million tonnes) will be nitrate fertilizers (FAO 2019). However, there are compelling economic and environmental reasons to reduce N fertiliser use in

Received 2 December, 2020 Accepted 2 April, 2021

Marcus GRIFFITHS, E-mail: mgriffiths@danforthcenter.org;
Correspondence Darren M. WELLS, Tel: +44-115-9516373,
E-mail: darren.wells@nottingham.ac.uk

© 2022 CAAS. Published by Elsevier B.V. This is an open access article under the CC BY-NC-ND license (<http://creativecommons.org/licenses/by-nc-nd/4.0/>).
doi: 10.1016/S2095-3119(21)63700-0

agriculture, particularly as the N fixing process is reliant on unsustainable fossil fuels (Dawson *et al.* 2008).

The availability of nutrients is spatially and temporally heterogeneous in soil (Lark *et al.* 2004; Miller *et al.* 2007), so roots need to forage for such resources. The spatial arrangement of the root system, called the root system architecture (RSA) (Hodge *et al.* 2009), has a profound effect on the uptake of nutrients and consequently the potential yield. Optimisation of the RSA can significantly improve the efficiency of resource acquisition, and in turn increase the yield potential of the crop. An improvement in N use efficiency (NUE) by just 1% could reduce fertiliser losses and save ~1.1 billion USD annually (Delogu *et al.* 1998; Kant *et al.* 2010).

Understanding the contribution of root traits to RSA and function is of central importance for improving crop productivity. However, roots are inherently challenging to study, leading to the wide use of artificial growth systems for plant phenotyping as they are generally high-throughput, allow precise control of environmental parameters and are easy to replicate. These phenotyping systems have been key for the generation of root phenotypic data for association mapping and uncovering the underlying genetic mechanisms (Ren *et al.* 2012; Clark *et al.* 2013; Atkinson *et al.* 2015; Zurek *et al.* 2015; Yang *et al.* 2020). Such seedling phenotyping approaches have revealed QTL for root system architectural traits on chromosome regions that have also been found for related traits in field trials (Bai *et al.* 2013; Atkinson *et al.* 2015). However, only a limited number of studies have directly compared seedling screens to mature root traits in the field and the overall results have been inconsistent. This inconsistency likely reflects the lack of environmental control in the field, the focus of seedling studies on the seminal root system and not the crown root system, and the fact that field approaches for RSA research are in need of further development (Watt *et al.* 2013; Rich *et al.* 2020).

For many cereal crops, understanding the genetic basis of RSA is complex due to their polyploid nature and large genome sizes. Therefore, quantitative trait loci (QTLs) analyses have been very useful for precisely linking phenotypes to regions of a chromosome. With the development of high-throughput RNA sequencing technology (RNA-seq), identified QTL can now be further dissected to the gene level. Using RNA-seq, a substantial number of genes and novel transcripts that are implicated in RSA control have been identified in various cereal crops, including rice, sorghum, maize and wheat (Oono *et al.* 2013; Gelli *et al.* 2014; Akpınar *et al.* 2015; Yu *et al.* 2015). To our knowledge, no other studies have identified genes related to nitrate response or root angle change in

wheat. The discovery of these genes and mechanisms are likely to be of agronomic importance, as they can then be implemented in genomics-assisted breeding programs to improve N-uptake efficiency in crops.

The aim of this study was to identify root traits and genes related to N uptake and plasticity in wheat. To achieve this, a germination paper-based system was used to phenotype a wheat doubled haploid (DH) mapping population under two N regimes. The nitrate-N levels were varied to determine the seedling responses to high- and low-affinity transport relevant concentrations similar to those that would be experienced in the field. Here we present the genomic regions and underlying genes that appear to control root size and root distribution responses to nitrate in wheat.

2. Materials and methods

2.1. Plant materials

A winter wheat doubled haploid mapping population comprised of 94 lines was used for root phenotyping. The population was derived from an F₁ plant derived from cultivars Savannah and Rialto (Limagrain UK Ltd., Rothwell, UK). Both parents are UK winter wheat cultivars on the AHDB recommended list. Savannah is a National Association of British & Irish Millers (NABIM) Group 4 feed cultivar first released in 1998. Rialto is a NABIM Group 2 bread-making cultivar first released in 1995. Previous field research found that Rialto had differential grain yield in low N field trials compared to Savannah, suggesting that it would make a promising population to characterize with limited root characterization in response to N (Gaju *et al.* 2011).

2.2. Seedling phenotyping

Wheat seedlings were grown using a high-throughput germination paper-based plant phenotyping system as described in Atkinson *et al.* (2015). Briefly, seedlings are grown inside a pouch consisting of a wetted sheet of germination paper (24 cm×30 cm) covered with black polythene film (Fig. 1). The pouches were suspended using a rack so that the bottom 3 cm of the pouch was submerged in a nutrient solution. During root system imaging, the black polythene film was simply removed to reveal the undisturbed root system (Fig. 1-B). Seeds from the Savannah×Rialto doubled haploid (S×R DH) mapping population were sieved to a seed size range of 2.8–3.35 mm based on the mean parental seed size. Seeds were surface sterilised in 5% (v/v) sodium hypochlorite for 12 min prior to three washes in dH₂O. Sterilised seeds

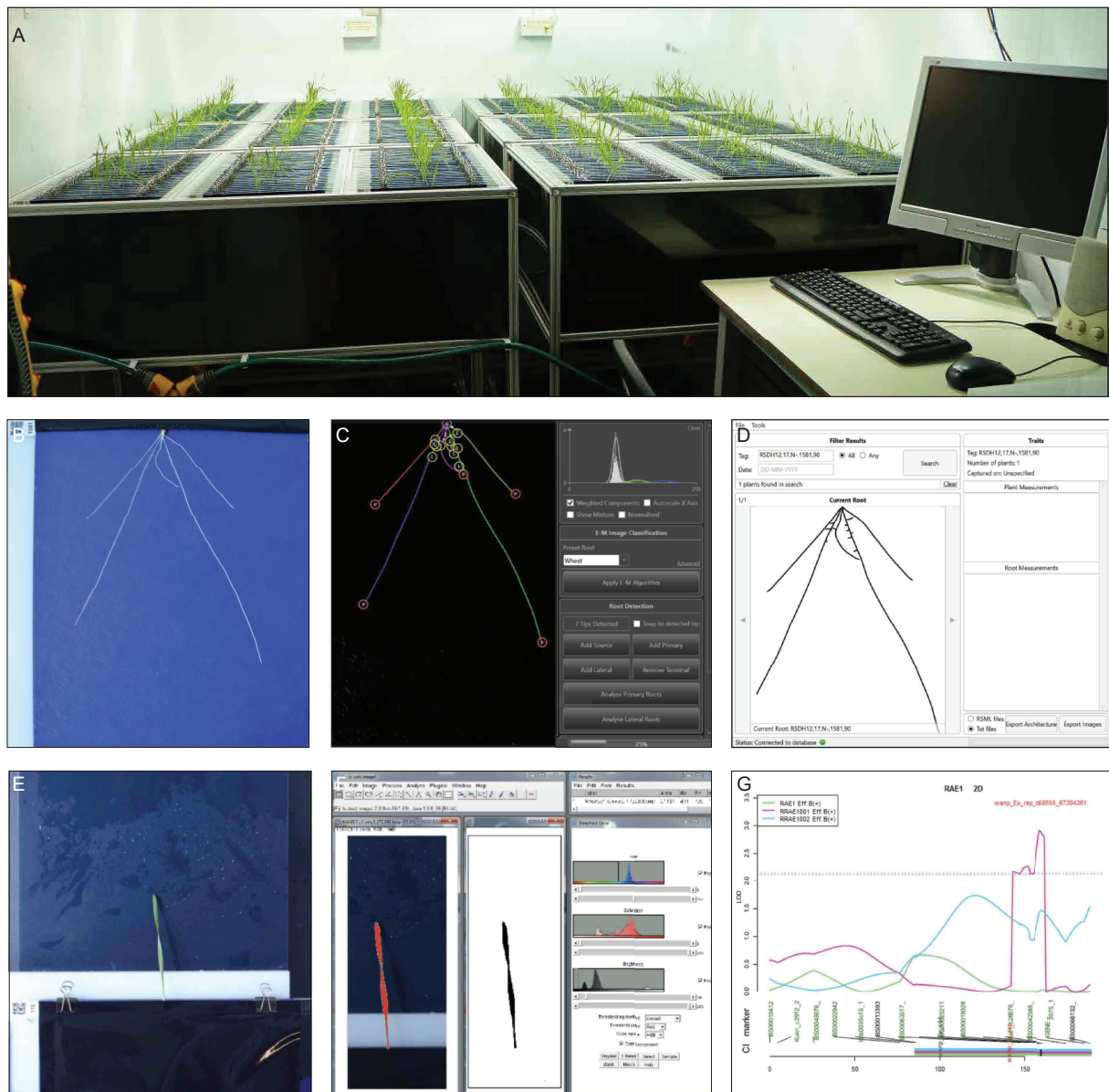


Fig. 1 High-throughput hydroponic phenotyping system for seedling root and shoot traits. A, growth assembly and plant imaging station. B, sample image of a wheat root grown on germination paper at 10 days after germination. C, root system extraction to the Root System Markup Language (RSML) database using RootNav Software. D, measurement of root traits from the RSML database. E, sample image of a wheat shoot at 10 days after germination. F, shoot image colour thresholding and shoot measurement using FIJI Software Package. G, example of a QTL peak extracted from phenotyping data and mapping data with R/qtl.

were laid on wet germination paper (Anchor Paper Company, St. Paul, MN, USA) and stratified at 4°C in a dark controlled-environment room for 5 days. After stratification, seeds were transferred to a controlled-environment room at 20/15°C, 12-h photoperiod, 400 μmol m⁻² s⁻¹ PAR and kept in a light-tight container. After 48 h, uniformly germinated seedlings with ~5 mm radicle length were transferred to vertically-orientated seedling pouches.

Seeds for 94 lines from the S×R DH mapping

population were grown hydroponically either in high nitrate (3.13 mmol L⁻¹ NO₃⁻, 0.75 mmol L⁻¹ NH₄⁺) or low nitrate (0.23 mmol L⁻¹ NO₃⁻, 0.75 mmol L⁻¹ NH₄⁺) modified Hoagland's solution (Appendix A). The experimental design was a randomised block comprised of the 94 genotypes split over 11 experimental runs with a target of 20 replications per genotype (*n*=8–36). The RSA of each seedling was extracted from the images and stored in Root System Markup Language (RSML; Lobet *et al.* 2015) using the root tracing software RootNav (Pound

et al. 2013). Root traits were quantified using RootNav standard functions and additional measurements as described in Atkinson *et al.* (2015). The shoot length and area were extracted from the shoot images using custom macros in the FIJI Software Package (Schindelin *et al.* 2012) (macro code available in Appendix B). Definitions for all extracted traits are given in Table 1. Analysis of variance of the raw plant data was conducted using the R package “lmerTest” (Kuznetsova *et al.* 2017) with random effects by experimental run. Broad-sense heritability (h^2) was calculated using the equation $h^2 = \sigma_g^2 / (\sigma_g^2 + \sigma_e^2)$, where σ_g^2 and σ_e^2 are the genetic and residual variances, respectively (Falconer 1996). A principal component analysis (PCA) and correlation matrices were applied using R Stats Package v3.6.2 and “FactoMineR” (Husson *et al.* 2019), by using the scaled mean values to explore the relationships between the traits and genotypes within the dataset. Finally, a correlation matrix was generated using the R Statistics package “corrplot” (Wei and Simko 2017), by using the raw plant data from both treatments to determine overall correlations between traits.

2.3. Quantitative trait locus mapping

Detection of QTL and the calculation of estimates for additive effects were conducted using the R Statistics package “R/qtl” (Broman *et al.* 2003). The map used was a high-density Savannah×Rialto iSelect map obtained from Wang *et al.* (2014) with redundant markers and markers closer than 0.5 cM stripped out, which reduced the number of effective markers from 46 977 to 9 239 (Appendix C). Average marker density by chromosome ranged between 0.16 and 4.23 markers per cM. Before QTL analysis, best linear unbiased predictions (BLUPs) were calculated for traits showing variance between experimental runs, and best linear unbiased estimations (BLUEs) were calculated for all other traits (Henderson 1975; Atkinson *et al.* 2015) (Appendix D). QTL were identified based on the composite interval mapping (CIM) *via* extended Haley-Knott regression (Haley and Knott 1992). The threshold logarithm of the odds (LOD) scores and effects were calculated by the 1 000×permutation test at the $P < 0.05$ level (Churchill and Doerge 1994). After the

Table 1 Definition of plant traits measured

Acronym	Definition	Software	Unit
RAE1	Angle of emergence between the outermost seminal roots measured at 30 px	RootNav	Degrees (°)
RAE1001	Angle of emergence between outermost pair of seminal roots measured at root tip	RootNav	Degrees (°)
RAE1002	Angle of emergence between innermost pair of seminal roots measured at root tip	RootNav	Degrees (°)
RAE2	Angle of emergence between innermost pair of seminal roots measured at 30 px	RootNav	Degrees (°)
RAE251	Angle of emergence between outermost pair of seminal roots measured at first quartile of total length	RootNav	Degrees (°)
RAE252	Angle of emergence between innermost pair of seminal roots measured at first quartile of total length	RootNav	Degrees (°)
RAE501	Angle of emergence between outermost pair of seminal roots measured at second quartile of total length	RootNav	Degrees (°)
RAE502	Angle of emergence between innermost pair of seminal roots measured at first quartile of total length	RootNav	Degrees (°)
RAE751	Angle of emergence between outermost pair of seminal roots measured at third quartile of total length	RootNav	Degrees (°)
RAE752	Angle of emergence between innermost pair of seminal roots measured at third quartile of total length	RootNav	Degrees (°)
RAE951	Angle of emergence between outermost pair of seminal roots measured at 95 px	RootNav	Degrees (°)
RAE952	Angle of emergence between innermost pair of seminal roots measured at 95 px	RootNav	Degrees (°)
RCH	Convex hull-area of the smallest convex polygon to enclose the root system	RootNav	mm ²
RCHCX	Convex hull centroid-horizontal co-ordinate	RootNav	mm
RCHCY	Convex hull centroid-vertical co-ordinate	RootNav	mm
RCMX	Root centre of mass-horizontal co-ordinate	RootNav	mm
RCMY	Root centre of mass-vertical co-ordinate	RootNav	mm
RLC	Number of lateral roots	RootNav	Dimensionless (count)
RMD	Maximum depth of the root system	RootNav	mm
RMW	Maximum width of the root system	RootNav	mm
RWDR	Width-depth ratio (RMW/RMD)	RootNav	Dimensionless (ratio)
RSC	Number of seminal roots	RootNav	Dimensionless (count)
RTLA	Total length of all roots	RootNav	mm
RTLL	Total length of lateral roots	RootNav	mm
RTLS	Total length of seminal roots	RootNav	mm
SA	Shoot area	FIJI	mm ²
SH	Shoot height	FIJI	mm

analysis, an additional threshold was applied for declaring the presence of a QTL with a minimum LOD score of 2.0. Confidence intervals for the identified QTLs were calculated using 1.5-LOD support intervals in which the LOD score is within 1.5 U of its maximum. The annotated linkage map was generated using the R Statistics package “LinkageMapView” (Ouellette *et al.* 2018).

2.4. RNA-sequencing of candidate QTL

RNA-seq was used to identify underlying genes for a candidate seminal root angle QTL (LOD 3.0) located on chromosome 2D, which was found under low nitrate conditions. One sample group was comprised of lines that had the candidate QTL (Group A: lines 17, 20, 36, 68) and the second sample group did not have the QTL (Group B: lines 6, 8, 11, 52). All pooled root samples of plants grown under low nitrate conditions were collected at the same time and immediately frozen using liquid nitrogen and stored at -80°C . Each sample group had four RNA biological replicates, where each replicate was a pool of roots from three plants per line (12 plants per RNA sample). Total RNA was isolated from 500–1 000 mg of homogenised root tissue (TRIzol reagent, Thermo Fisher Scientific, USA). RNA quality and purity were determined using a NanoDrop™ 2000c, with values of $500\text{ ng }\mu\text{L}^{-1}$ or higher accepted. Illumina 75 bp Paired-End Multiplexed RNA sequencing was performed using a NextSeq 500 by Source Bioscience (Nottingham, UK).

Differential gene expression analysis was conducted using the IWGSC RefSeq v1.1 assembly (IWGSC 2018) (http://plants.ensembl.org/Triticum_aestivum/) and the TGAC v1 Chinese Spring reference sequence (Clavijo *et al.* 2017). Raw sequencing reads were trimmed for adapter sequences and for regions where the average quality per base dropped below 15 (Trimmomatic version 0.32) (Bolger *et al.* 2014). After trimming, reads below 40 bp were eliminated from the dataset. Trimmed reads were aligned to the reference sequence assembly using splice-aware aligner HISAT2 (Pertea *et al.* 2016). Uniquely mapped reads were selected, and duplicate reads were filtered out. Unmapped reads across all samples were assembled into transcripts using MaSuRCA Software and sequences 250 bp or larger were taken forward (Zimin *et al.* 2013). Unmapped reads were re-aligned to these assembled transcripts individually and added to their sample specific reads, while the assembled transcripts were combined with the reference sequence and GTF annotation for downstream investigations. StringTie Software was used to calculate gene and transcript abundances for each sample across the analysis-specific annotated genes (Pertea

et al. 2016). The sequencing read depth and alignment statistics are provided in Appendix E. Finally, DESeq was used to visualise the results and identify differential expression between samples (Anders and Huber 2010). Differentially expressed genes were compared between the IWGSC RefSeq v1.1 and TGAC v1 reference assemblies to identify overlap using BLAST (BLASTN, e-value $1\text{e}-05$, identity 95%, minimum length 40 bp) (Altschul *et al.* 1990). The top matches for each gene between the reference sequences were used to allow an integrative and comprehensive annotation of genes. Gene Ontology (GO) analysis was performed with the latest genome for *Triticum aestivum* (IWGSC RefSeq v1.1 assembly) in g:Profiler (Raudvere *et al.* 2019) using the tailor made algorithm g:SCS for computing multiple testing correction for *P*-values gained from the GO enrichment analysis. A *P*-value threshold of 0.05 was applied, with only those results passing this threshold reported.

2.5. Phylogenetic analysis

A phylogenetic analysis of protein families was conducted to compare the protein sequences of proton-dependent oligopeptide transporter (NPF) families (also known as the NRT1/PTR family) from *Arabidopsis thaliana*, *Oryza sativa* L. and *T. aestivum* L. *Arabidopsis thaliana* sequences were obtained from (Léran *et al.* 2014). Using the latest genomes for *T. aestivum* (IWGSC RefSeq v1.1 assembly) and *O. sativa* (MSU Release 7.0, Kawahara *et al.* 2013, <https://phytozome.jgi.doe.gov/>), an HMM profile search was conducted (Krogh *et al.* 2001). The resulting list of proteins was scanned using Pfam (El-Gebali *et al.* 2019). Only single gene models of candidate genes with PTR2 domains were retained. The protein sequences were used to generate a maximum-likelihood tree using the Software RAXML (Stamatakis 2014). The exported tree file (.NWK) was then visualised using the R package “ggtree” (Yu *et al.* 2017) and used for phylogenetic tree construction.

2.6. Data availability statement

The RNA-seq dataset (study PRJEB40436) is available from the European Nucleotide Archive (<http://www.ebi.ac.uk/ena/data/view/PRJEB40436>).

3. Results

3.1. Phenotypic variation in a wheat doubled haploid population for seedling traits and nitrate effects

Seedlings for 92 lines of the S×R DH mapping population and the parents were grown hydroponically in a controlled-

environment chamber under high and low nitrate treatments (Fig. 1). The roots and shoots of each seedling were individually imaged 10 days after germination resulting in 6 924 images. The results of ANOVA indicated that the variances for the genotype effects for all investigated seedling traits were highly significant ($P < 0.001$) (Appendix F). Across the wheat population, many of the root size and root distribution traits were found to be nitrate treatment-dependent. Interestingly, no significant differences were observed across the population for total root length in response to the nitrate treatment, however, the root class distribution between lateral ($P < 0.001$) and seminal ($P < 0.01$) root length was significantly affected with a G×N-treatment interaction ($P < 0.001$). In addition, seminal root angle traits and width–depth related traits had significant nitrate treatment effects ($P < 0.05$). The seedling traits measured were also highly heritable, with heritability scores for root length and count traits between 0.78–0.97, root distribution traits between 0.40–0.97, root angle traits between 0.51–0.84 and shoot traits between 0.77–0.84 (Appendix F).

3.2. Wheat root phenotypic traits segregate into two distinct clusters by size and distribution

For the S×R DH population and the parents, a PCA was conducted to explore the relationships among the root phenotypic traits (Fig. 2-A). N treatment did not affect

the PCA trait loadings or correlations between the traits (Appendix G), so the analyses were conducted for both treatments together. Over 71% of the trait variation could be explained by the first two principal components, and 90% of the trait variation could be explained by the first six principal components. The loadings were mostly split between root size related traits and root distribution traits (Fig. 2-A). A correlation matrix of the whole dataset demonstrated a strong correlation between root size related traits and root distribution related traits (Fig. 2-B). Of all the plant traits measured, the width–depth ratio traits were found to be positively correlated with the greatest number of traits from both trait groups, plant size and root distribution. In addition, the correlation analysis also highlighted negative associations between root size and angle traits.

3.3. Identification of novel root QTLs in the S×R DH population

Using normalized phenotypic data with a high-density Savannah×Rialto iSelect map, a total of 59 QTLs were discovered for seedling traits, among which 41 QTLs had positive effect alleles coming from Savannah and 18 from Rialto (Fig. 3; Table 2). QTLs were found on chromosomes 1A, 1B, 2D, 3B, 4D, 6D, 7A, and 7D, with 25 QTLs located on 6D. For the rooting traits, a total of

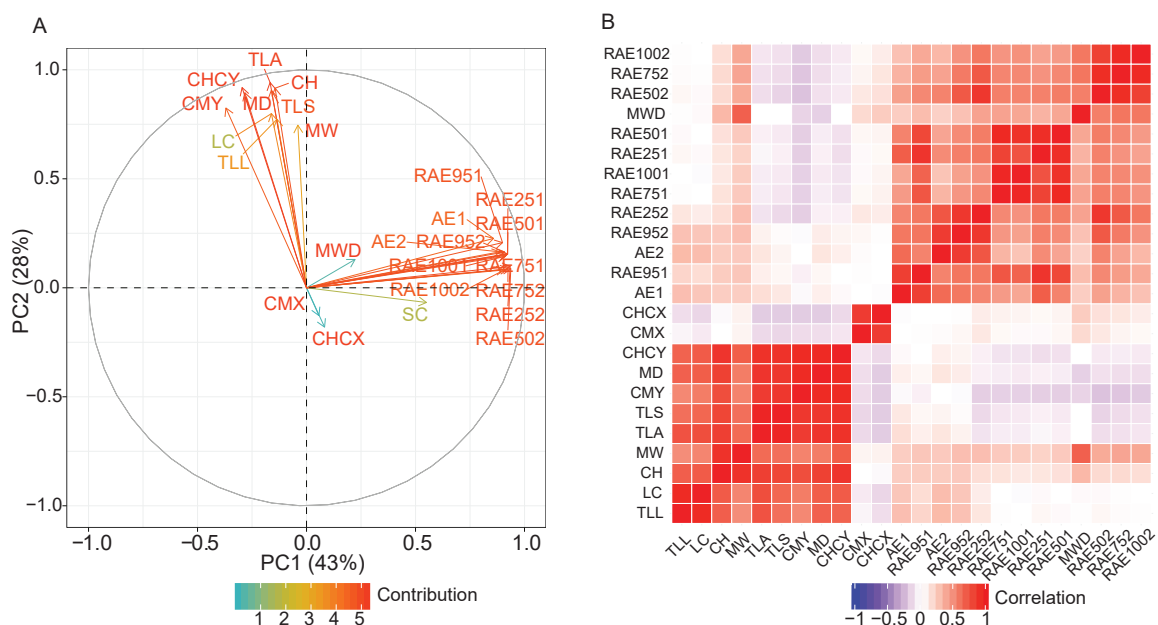


Fig. 2 Principal component analysis and correlation of extracted root traits for the Savannah×Rialto doubled haploid (S×R DH) population and parents under high and low nitrate regimes. A, PCA ordination results for the Savannah×Rialto doubled haploid (S×R DH) population and parents under high and low nitrate regimes. Arrows indicate directions and contributions of loadings for each trait. B, correlation matrix of extracted root traits averaged between nitrate treatments. Correlations are colour-coded from strong positive correlation in red to strong negative correlation in blue, with no correlation shown in white.

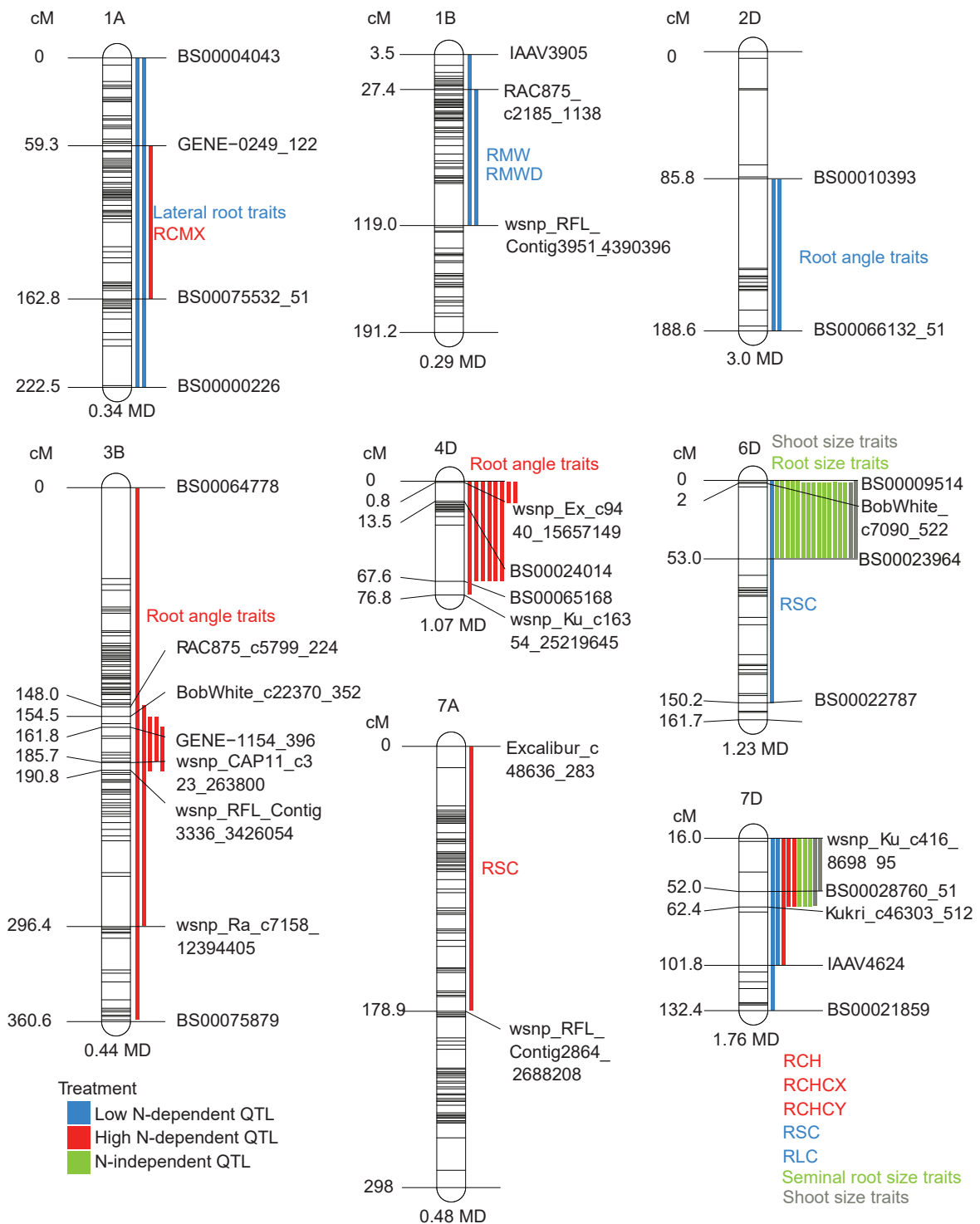


Fig. 3 Molecular linkage map showing the positions of QTLs detected in the Savannah×Rialto doubled haploid (S×R DH) population grown in hydroponics (LOD (logarithm of the odds value)>2.0). Shoot QTLs found in the low N study are shown in grey. Marker density (MD) per chromosome is displayed as average cM per marker.

55 QTLs were found across the two nitrate treatments, 23 of which were identified under the low nitrate treatment and 32 under the high nitrate treatment. Nine root QTLs were found to be only present in the low nitrate treatment,

while 18 root QTLs were found only in the high nitrate treatment and 14 root QTLs (28 total) were present in both nitrate treatments. The trait ANOVA results also support the notion that the root QTLs found are nitrate condition

dependent. Phenotypic variation explained by the QTLs varied from 3.8 to 82.9%. Of the QTLs found, there appear to be 13 underlying root QTLs, with many root size and root distribution class traits co-localized at the same chromosome region. Two QTLs involved in shoot size traits, which were identified on chromosomes 6D and 7D under low N, were colocalized with the corresponding QTLs of root size traits. N-dependent QTLs of some traits on chromosomes 6D and 7D were colocalized with N-independent QTLs of other root size traits. Among QTLs associated with nitrate treatment, QTLs for root size were found on chromosomes 1A, 6D and 7D and for root angle on chromosomes 2D, 3B and 4D. Of these regions, a candidate root angle QTL (RAE1001) residing on chromosome 2D was investigated further. For this QTL, a positive allele from Rialto conferred a root angle change in the low nitrate treatment that co-localised with other root angle traits and explained 14.3% of the phenotypic variation with a broad peak confidence region (25 cM) (Table 2).

3.4. Differentially regulated candidate genes for a root angle QTL identified by RNA-seq analysis

The lines for the RNA-seq analysis were selected based on the largest observed phenotypic differences for the trait associated with a root angle QTL located on chromosome 2D (RAE1001), which was found under low nitrate conditions. The DH population showed transgressive

segregation with trait values more extreme than those of the parents (Fig. 4-A). Under low nitrate, there was a 30° difference in root angle ($P < 0.001$) between the extremes of the population, with four lines of each subsequently used for RNA-seq (Fig. 4-B and C). The sample groups also differed in their response to N, with a significantly steeper root angle under low-nitrate in one of the groups ($P < 0.05$) (Fig. 4-B).

One sample group was comprised of lines that had the candidate QTL with a positive effect from the parent Rialto (Group A: lines 17, 20, 36, 68), and the second sample group had the parental origin from Savannah (Group B: lines 6, 8, 11, 52). As there was no single clear enriched region for the root QTL located on chromosome 2D, the whole chromosome was considered for differential gene expression analysis. A total of 3 299 differentially expressed genes were identified in the analysed groups. We then focused on the identification of genes that were consistently overexpressed in Group A compared to Group B, as they could be driving the QTL. A total of 1 857 differentially expressed genes showed significant ($P < 0.05$) up-regulation in Group A (with the QTL) compared to Group B (without QTL) considering all four biological replicates in each case. Of these, 88 gene candidates resided on chromosome 2D. In addition, MaSuRcA transcript assemblies were considered that were identified as significantly ($P < 0.05$) up-regulated in Group A compared Group B on chromosome 2D, bringing the total to 93 (88 plus five) differentially expressed candidate sequences

Table 2 QTLs for wheat seedling traits detected in the Savannah×Rialto doubled haploid (S×R DH) population grown in hydroponics (LOD>2.0)¹⁾

Trait	Treat ²⁾	QTL	Confidence interval (CI) markers	CI begin	CI end	Peak (cM)	LOD	Additive effect	PVE (%)
RTL A	LN	6D	BobWhite_c7090_522–BS00023964	2	53	5.0	27.4	–229	65.0
		7D	w SNP_Ku_c416_869895–BS00028760_51	16	52	26.0	8.4	–107	11.3
	HN	6D	BobWhite_c7090_522–BS00023964	2	53	4.4	23.0	–201	57.4
		7D	w SNP_Ku_c416_869895–BS00028760_51	16	52	27.0	8.7	–111	14.3
RTL S	LN	6D	BobWhite_c7090_522–BS00023964	2	53	5.0	33.5	–198	70.5
		7D	w SNP_Ku_c416_869895–BS00028760_51	16	52	26.0	11.3	–86	12.1
	HN	6D	BobWhite_c7090_522–BS00023964	2	53	4.4	24.8	–168	59.9
		7D	w SNP_Ku_c416_869895–BS00028760_51	16	52	27.0	9.4	–91.2	14.4
RTL L	LN	1A	BS00004043–BS00000226	0	222.5	215.0	2.3	–9.0	6.2
		6D	BobWhite_c7090_522–BS00023964	2	53	8.0	13.4	–31.2	48.0
	HN	6D	BS00009514–BS00023964	0	53	4.4	6.3	–32.8	28.0
RAE1	HN	3B	BobWhite_c22370_352–w SNP_RFL_Contig3336_3426054	154.5	185.7	178.8	2.2	–11.0	10.8
RAE2	HN	3B	GENE-1154_396–w SNP_RFL_Contig3336_3426054	161.8	190.8	178.8	2.8	–8.2	13.3
RLC	LN	1A	BS00004043–BS00000226	0	222.5	216.0	4.9	–2.4	8.6
		6D	BobWhite_c7090_522–BS00023964	2	53	5.0	19.6	–9.4	52.8
		7D	w SNP_Ku_c416_869895–BS00028760_51	16	52	22.0	6.0	–4.4	10.9
	HN	6D	BS00009514–BS00023964	0	53	4.4	8.8	–8.5	36.5

(Continued on next page)

Table 2 (Continued from preceding page)

Trait	Treat ²⁾	QTL	Confidence interval (CI) markers	CI begin	CI end	Peak (cM)	LOD	Additive effect	PVE (%)
RSC	LN	6D	BS00009514–BS00022787	0	150.2	4.4	3.2	0.2	13.1
		7D	wsnp_Ku_c416_869895–IAAV4624	16	101.8	23.0	3.8	–0.2	15.8
	HN	7A	Excalibur_c48636_283–wsnp_RFL_Contig2864_2688208	0	178.9	12.0	2.9	0.2	13.7
RCH	LN	6D	BobWhite_c7090_522–BS00023964	2	53	4.4	31.1	–8464	80.0
		HN	6D	BobWhite_c7090_522–BS00023964	2	53	4.4	18.4	–7118
		7D	wsnp_Ku_c416_869895–Kukri_c46303_512	16	62.4	34.0	4.2	–3309	8.3
RMW	LN	1B	IAAV3905–wsnp_RFL_Contig3951_4390396	3.5	119	12.5	3.6	–8.9	5.0
		6D	BobWhite_c7090_522–BS00023964	2	53	4.4	26.7	–48.5	72.8
	HN	4D	wsnp_Ex_c9440_15657149–wsnp_Ku_c16354_25219645	0.8	76.8	23.9	3.1	10.8	7.1
RMD	LN	6D	BS00009514–BS00023964	0	53	4.4	16.4	–36.2	54.6
		7D	BobWhite_c7090_522–BS00023964	2	53	4.4	31.5	–71.4	75.1
	HN	6D	wsnp_Ku_c416_869895–BS00021859	16	132.4	27.0	3.7	–20.6	3.8
RMWD	LN	6D	BobWhite_c7090_522–BS00023964	2	53	4.4	21.8	–60.3	58.8
		7D	wsnp_Ku_c416_869895–BS00028760_51	16	52	30.0	5.2	–26.6	8.6
	HN	1B	RAC875_c2185_1138–BobWhite_c23617_167	27.4	119	86.2	2.2	–0.03	10.5
RCMX	LN	4D	wsnp_Ex_c9440_15657149–BS00065168	0.8	67.6	4.8	3.1	0.1	14.6
		HN	6D	BS00009514–BS00023964	0	53	6.0	2.3	1.6
	HN	1A	GENE-0249_122–BS00075532_51	59.3	162.8	145.0	4.1	–1.7	16.6
RCMY	LN	6D	BS00009514–BS00023964	0	53	22.0	4.0	1.5	16.3
		HN	6D	BobWhite_c7090_522–BS00023964	2	53	4.4	31.9	–23.1
	HN	6D	BobWhite_c7090_522–BS00023964	0	53	4.4	19.5	–19.3	63.5
RCHCX	LN	6D	BS00009514–BS00023964	0	53	4.4	2.3	2.5	11.2
		HN	6D	BS00009514–BS00023964	0	53	18.0	3.2	2.14
		7D	wsnp_Ku_c416_869895–IAAV4624	16	101.8	21.0	3.2	2.6	13.1
RCHCY	LN	6D	BobWhite_c7090_522–BS00023964	2	53	4.4	34.1	–40.0	82.9
		HN	3B	BS00064778–BS00075879	0	360.6	216.2	4.9	7.11
		6D	BobWhite_c7090_522–BS00023964	2	53	4.4	25.0	–33.9	62.1
RAE951	LN	7D	wsnp_Ku_c416_869895–Kukri_c46303_512	16	62.4	32.0	5.8	–14.4	8.2
		HN	3B	RAC875_c5799_224–wsnp_Ra_c7158_12394405	148	296.4	178.8	2.8	–7.7
	HN	3B	BobWhite_c22370_352–wsnp_CAP11_c323_263800	154.5	185.7	178.8	3.6	–7.7	17.0
RAE252	HN	4D	wsnp_Ex_c9440_15657149–BS00065168	0.8	67.6	0.8	2.8	6.5	13.4
RAE501	HN	4D	wsnp_Ex_c9440_15657149–BS00065168	0.8	67.6	0.8	2.9	6.3	14.0
RAE502	HN	4D	wsnp_Ex_c9440_15657149–BS00065168	0.8	67.6	0.8	3.0	6.4	14.2
RAE751	LN	2D	BS00010393–BS00066132_51	85.8	188.6	160.0	2.6	5.1	12.5
		HN	4D	wsnp_Ex_c9440_15657149–BS00024014	0.8	13.5	0.8	2.9	6.3
RAE752	HN	4D	wsnp_Ex_c9440_15657149–BS00065168	0.8	67.6	0.8	2.1	5.3	10.4
RAE1001	LN	2D	BS00010393–BS00066132_51	85.8	188.6	160.0	3.0	5.5	14.3
		HN	4D	wsnp_Ex_c9440_15657149–BS00024014	0.8	13.5	0.8	2.4	6.0
SA	LN	6D	BobWhite_c7090_522–BS00023964	2	53	8.0	24.4	–1.0	61.4
		7D	wsnp_Ku_c416_869895–	16	52	29.0	7.0	–0.6	10.6
SH	LN	6D	BS00009514–BS00023964	0	53	4.4	19.3	–0.6	54.5
		7D	wsnp_Ku_c416_869895–Kukri_c46303_512	16	62.4	31.0	6.0	–0.3	11.7

¹⁾ Trait units are given in Table 1, shoot data were collected for low nitrate conditions only; confidence interval markers, chromosome region of the QTL defined by two flanking markers; peak, genetic position of the QTL peak value; LOD, logarithm of the odds value; additive effect, additive effects of putative QTL, a positive value indicates that positive alleles are from Rialto, a negative value indicates that positive alleles are from Savannah; PVE, percentage of phenotypic variation explained by putative QTL.

²⁾ LN, low nitrate; HN, high nitrate.

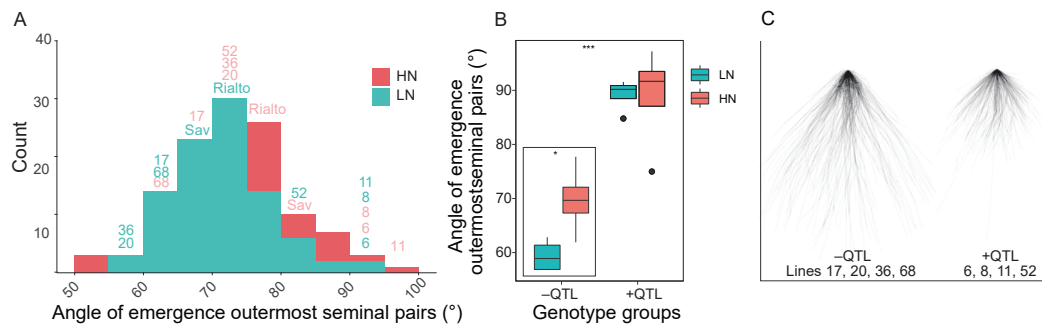


Fig. 4 Variation in seminal root angle (RAE1001) for the Savannah×Rialto doubled haploid (S×R DH) population under two nitrate regimes. A, distribution of means. Labeled non-parental lines were selected for RNA-seq. B, boxplot. C, overlay plot for the lines selected for RNA-seq with differential seminal root angle (RAE1001). +QTL, sample group was comprised of lines that had the candidate QTL with positive effect from Rialto; -QTL, sample group had the parental origin from Savannah. LN, low nitrate; HN, high nitrate. *, $P \leq 0.05$; ***, $P \leq 0.001$.

(Appendix H). The inclusion of *de novo* assembled transcript sequences in the analysis accounts for varietal specific genes that are not present in the Chinese Spring reference sequences. The sequencing read depth and alignment statistics are provided in Appendix E. Of the 93 differentially expressed candidate sequences listed

in Appendix H, 17 candidate genes were consistently expressed across the Group A replicates versus zero reads mapping in one or more Group B replicates, and the former were therefore considered as our primary candidates (Table 3). Another 1 442 differentially expressed genes showed significant ($P < 0.05$) down-

Table 3 Candidate genes for seminal root angle QTL located on chromosome 2D that were consistently expressed across the Group A replicates vs. zero reads mapping in one or more Group B replicates¹⁾

Gene	Log ₂ fold change	Adjusted <i>P</i> -value (<i>q</i> -value)	Functional annotation
<i>TraesCS2D02G088100</i>	1.29	0.036	C2H2-type zinc finger
<i>TraesCS2D02G108500</i>	1.38	0.026	Peroxidase
<i>TraesCS2D02G129100</i>	1.36	0.036	Legume lectin domain
<i>MSTRG.42598 (TGACv1)</i>	1.31	0.041	Unknown
<i>TraesCS2B02G126600</i>	2.21	9.5E-06	Unknown
<i>TraesCS6A02G175000</i>	1.66	0.002	Nuclear pore complex scaffold, nucleoporin
<i>TraesCS2D02G270000</i>	1.66	0.002	Helix-loop-helix DNA-binding domain
<i>TraesCS2D02G330200</i>	1.44	0.013	Unknown
<i>TraesCS2A02G111200</i>	2.12	2.5E-05	Kelch motif
<i>TraesCS2D02G344400</i>	1.45	0.013	Unknown
<i>TraesCS2D02G348400</i>	1.88	3.6E-04	NPF4
<i>MSTRG.40366 (TGACv1)</i>	2.02	8.9E-05	Unknown
<i>TraesCS4B02G057100</i>	1.48	0.013	Unknown
<i>TraesCS2D02G441300</i>	1.29	0.037	AAA domain UvrD/REP helicase N-terminal domain
<i>TraesCS2D02G487000</i>	1.53	0.008	DUF wound-responsive family protein
<i>TraesCS2D02G509700</i>	1.73	0.002	Peroxidase
<i>TraesCS2D02G511200</i>	1.41	0.025	Peroxidase
<i>TraesCS2D02G408400LC</i>	-4.74	1.07E-35	Protein FAR1-RELATED SEQUENCE 5
<i>MSTRG.38813 (TGACv1)</i>	-2.77	2.18E-09	Unknown
<i>MSTRG.41948 (TGACv1)</i>	-2.79	1.91E-09	AT hook motif DNA-binding
<i>MSTRG.40021 (TGACv1)</i>	-4.21	8.79E-26	Syntaxin-61
<i>MSTRG.41827 (TGACv1)</i>	-3.05	1.14E-11	Unknown
<i>MSTRG.41606 (TGACv1)</i>	-5.55	1.04E-51	Unknown
<i>MSTRG.40222 (TGACv1)</i>	-3.03	1.28E-11	Unknown
<i>MSTRG.42196 (TGACv1)</i>	-5.71	9.87E-59	Unknown
<i>MSTRG.41343 (TGACv1)</i>	-3.97	3.83E-22	Unknown
<i>MSTRG.40513 (TGACv1)</i>	-3.22	2.31E-13	Unknown
<i>TraesCS2D02G323600</i>	-4.69	5.07E-33	ATP-dependent RNA helicase SUPV3L1

¹⁾ Gene naming conventions are according to IWGSC RefSeq v1.1. Genes that are present on a chromosome other than chromosome 2D represent variations between the IWGSC RefSeqv1.1 and the TGACv1 assembly.

regulation in Group A (with the QTL) compared to Group B (without QTL). Of these, 65 were annotated as residing on chromosome 2D (Appendix H). Eleven genes from this set that were consistently expressed across the Group B replicates, versus zero reads mapping in one or more Group A replicates, were added to our primary candidate list (Table 3).

Functional categories for the significantly up- and down-regulated genes between contrasting sample groups for a root QTL found under low nitrate conditions were evaluated using g:profiler. For terms relating to biological processes, there were 58 up-regulated terms that had the same lowest *P*-value, including “nitrogen compound metabolic process”, “cellular nitrogen compound metabolic process”, “regulation of nitrogen compound metabolic process” and “cellular nitrogen compound biosynthetic process” (Fig. 5). For the down-regulated terms, three of the top 10 terms were “nitrogen compound metabolic process”, “organonitrogen compound metabolic process” and “cellular nitrogen compound metabolic process” (Fig. 5). The complete list of enriched GO terms for molecular function, biological process and cellular component is available in Appendix I. For the candidate root angle QTL found under low nitrate conditions (RAE1001), there were several N-related biological processes which were up- and down-regulated between the sample groups. In addition, within the candidate gene list, an up-regulated NPF family gene,

TraesCS2D02G348400, was identified which was consistently expressed across Group A and zero reads mapping in Group B. As this gene was expressed at low nitrate and located within the identified QTL interval, *BS00010393–BS00066132_51*, the function of this gene was investigated. A phylogenetic analysis of protein families was conducted which compared the NPF family protein sequences of *A. thaliana*, *O. sativa* and *T. aestivum* (Appendix J). A total of 53 *A. thaliana* proteins, 130 *O. sativa* proteins and 391 *T. aestivum* proteins were aligned using MUSCLE with 1000 bootstrap interactions and 20 maximum likelihood searches (Edgar 2004). The candidate *T. aestivum* protein *TraesCS2D02G348400* is situated in a monocot specific sub-clade within the NPF4 clade (Fig. 6). This clade includes *A. thaliana* NPF members AtNPF4.1, AtNPF4.2, AtNPF4.3, AtNPF4.4, AtNPF4.5, AtNPF4.6, and AtNPF4.7. In addition, the candidate protein is closely related to a rice nitrate (chlorate)/proton symporter protein LOC_Os04g41410.

4. Discussion

Root system architecture is an important agronomic trait since the growth, development and spatial distribution of the root system affects the extent of available soil resources that a plant can capture. However, roots are challenging to phenotype in soil without disturbing the spatial arrangement, and therefore non-destructive root

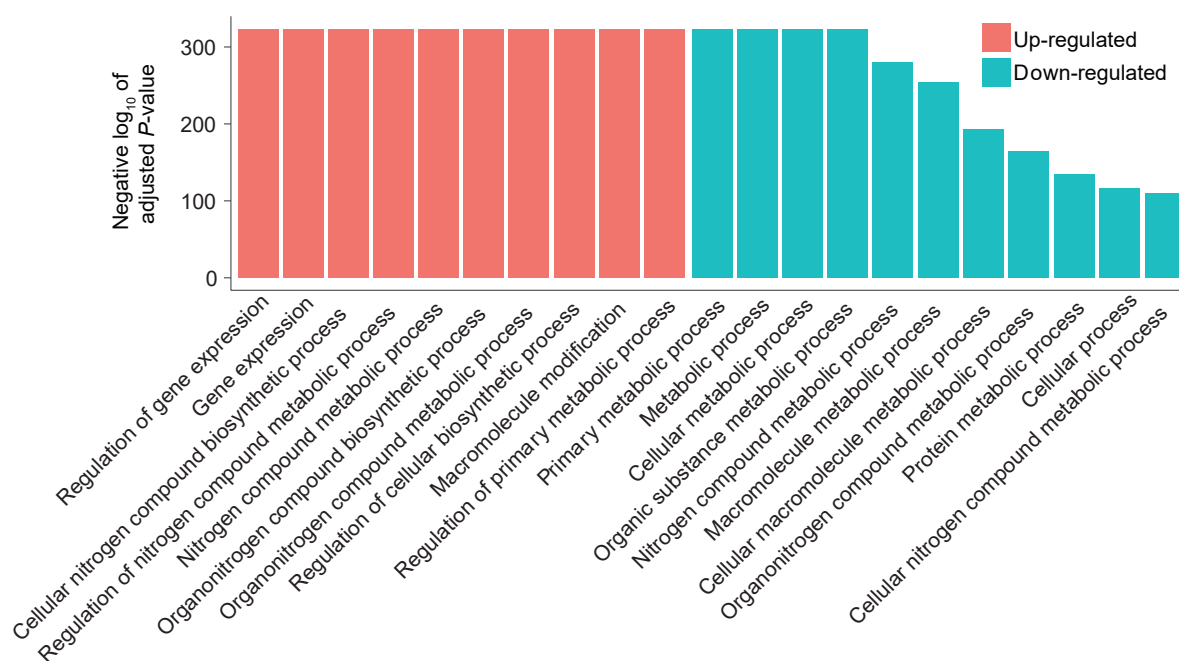


Fig. 5 Gene Ontology (GO) enrichment analysis for the top Biological process GO terms with the lowest *P*-values for up- and down-regulated genes in the sample group with a candidate seminal root angle QTL compared to the group without the QTL.

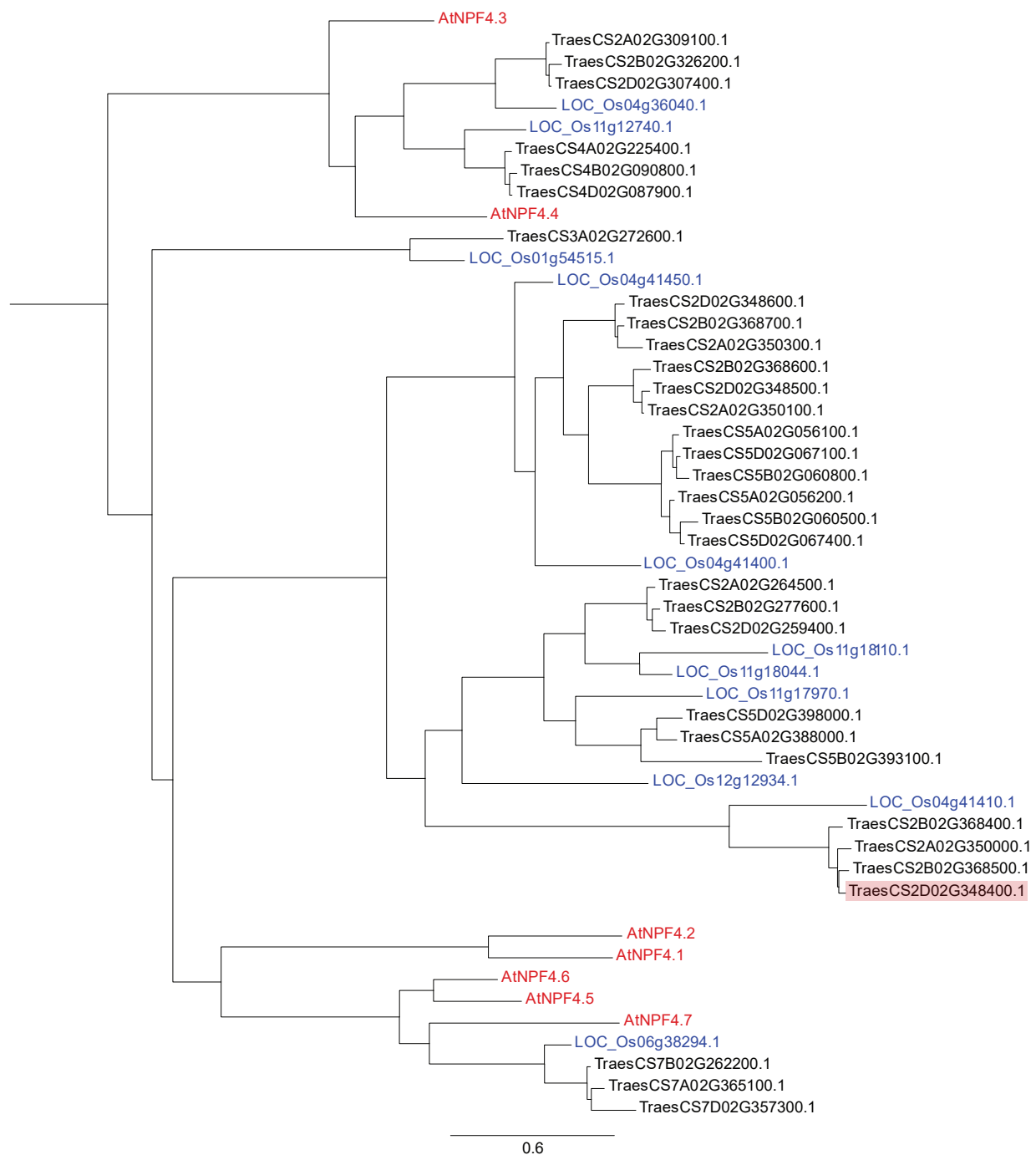


Fig. 6 Phylogenetic tree of protein families comparing the protein sequences of nitrate transporter 1/peptide transporter (NPF) family proteins from *Arabidopsis thaliana*, *Oryza sativa* L. and *Triticum aestivum* L. to an identified candidate *T. aestivum* protein. The candidate *T. aestivum* protein is situated in a monocot-specific outgroup within an NPF4 protein clade (highlighted in red). Branch lengths are proportional to substitution rate.

phenotyping systems such as germination paper screens and X-ray CT are invaluable tools for such work (Mooney *et al.* 2012; Bai *et al.* 2013; Atkinson *et al.* 2015). In this study, a germination paper-based system was used to phenotype a wheat DH mapping population under two nitrate-N regimes as this is a suitable approach for

population-size root phenotyping with precise control of nutrition.

Within the S×R DH mapping population, significant genotypic and nitrate treatment dependent phenotypic variation was observed in seedling traits (Appendix D). Overall, the seedling traits could be separated into

two main groups of related traits for root size and root distribution. In the root size trait group, the population had significant nitrate responsive plasticity in root length distribution. Interestingly, the root class lengths of seminal and lateral roots were significantly affected by nitrate treatment, yet the overall total root lengths were not significantly different. The root distribution-related trait group appeared to be the most responsive to nitrate treatment in this physiological screen using the S×R DH mapping population. Both root length distribution and root angle are widely regarded as important traits that are plastic to abiotic stimuli, such as low N or drought, as a plant can change the root foraging distribution in the soil to find such resources (Trachsel *et al.* 2013; Ho *et al.* 2018).

The use of high-throughput methods for growth and phenotyping enabled a whole wheat DH population to be scored for root and shoot traits and the data could be mapped to underlying chromosome regions by QTL analysis. Nitrate plasticity is a likely component of these QTLs which were only detected in one of the nitrate treatments. In addition, four QTLs were found for shoot size traits on chromosomes 6D and 7D in the low nitrate conditions (LOD>2.0) (Fig. 3; Table 2). In the literature, some studies have described QTL on regions associated with those found in this study for root and shoot seedling traits. In this study, it was found that the region on chromosome 1A is associated with lateral root traits under low nitrate conditions. Interestingly, chromosome 1A has been previously associated with lateral root length in wheat and rice (Ren *et al.* 2012; Beyer *et al.* 2018; Roselló *et al.* 2019). Therefore, there are likely underlying genes on chromosome 1A which are related to resource foraging as they were found to affect root plasticity, tolerance and/or lateral root development, resulting in an increase in grain yield in low input agricultural systems (An *et al.* 2006; Landjeva *et al.* 2008; Guo *et al.* 2012; Ren *et al.* 2012; Liu *et al.* 2013; Sun *et al.* 2013; Zhang *et al.* 2013; Good *et al.* 2017). This chromosome 1A region has also been correlated to nitrate uptake in S×R DH field trials (Atkinson *et al.* 2015), which would make this co-localized chromosome region an important candidate for further study regarding the potential association between root traits and N uptake. In this study, root angle QTLs on chromosomes 2D, 3B and 4D were also identified in the low nitrate conditions. QTLs on these chromosomes have been described in other studies, yet very few of them have measured root angle or distribution traits. In comparison with other studies that found root QTLs on chromosome 2D, it appears there may be an underlying gene or number of genes for seminal root development

and/or plasticity (An *et al.* 2006; Liu *et al.* 2013; Zhang *et al.* 2013). On chromosome 3B, other studies have found QTLs affecting root size and stress related traits or genes related to N plasticity, uptake and mobilisation (An *et al.* 2006; Habash *et al.* 2007; Guo *et al.* 2012; Bai *et al.* 2013; Zhang *et al.* 2013; Roselló *et al.* 2019). On chromosome 4D, other studies have also found QTLs that indicate an underlying root development and/or root plasticity gene which may be affecting the root angle or distribution change (Bai *et al.* 2013; Zhang *et al.* 2013).

A seminal root angle QTL (LOD 3.0) on chromosome 2D found under low nitrate conditions was targeted for transcriptomic analysis. Significant GO enrichments in N-related biological processes were found in the chromosome region of lines with the QTL compared to those without, indicating a differential low nitrate response in these lines. A total of 17 candidate up-regulated genes and 11 down-regulated genes were identified residing on chromosome 2D (Table 3). A detailed list of the genes identified is given in Appendix G. Two of the three genes with the highest log changes, plus four others, have unknown functions. Point mutation detection and mutant generation with TILLING, CRISPR/Cas9, or RNAi represent the next step in functionally characterising these genes in wheat. A promising candidate from the root transcriptomic analyses was an up-regulated nitrate transporter 1/peptide transporter (NPF) family gene, NPF4 (*TraesCS2D02G348400*), in lines that had the root angle QTL. In *A. thaliana* and *O. sativa*, NPF family genes have important roles in lateral root initiation, branching and responses to nitrate (Remans *et al.* 2006; Krouk *et al.* 2010; Fang *et al.* 2013). However, to date, no studies have reported genes controlling root angle changes in wheat. A phylogenetic analysis of protein families was conducted by comparing the protein sequences of *A. thaliana*, *O. sativa* and *T. aestivum* to the candidate protein. The candidate *T. aestivum* protein is situated in a monocot specific sub-clade within the NPF4 clade and is closely related to a rice nitrate (chlorate)/proton symporter protein (LOC_Os04g41410) (Fig. 6). Members of this clade are known for transporting the plant hormone abscisic acid (ABA) (AtNPF4.1 and AtNPF4.6) and have been shown to have low affinity nitrate transport activity (AtNPF4.6) (Huang *et al.* 1999; Kanno *et al.* 2012). ABA is known to be a key regulator in root hydrotropism, a process that senses and drives differential growth towards preferred water potential gradients (Takahashi *et al.* 2002; Antoni *et al.* 2016). As root angle is a determinant of root depth, further investigating the function of this gene is of agronomic importance for improving foraging capacity and the uptake of nitrate

from deep soil layers as seedling stage identified genes have been associated with yield-related traits (Xu *et al.* 2018).

5. Conclusion

In summary, we identified 59 QTLs using a wheat seedling hydroponic system, which included 27 for root traits found in nitrate treatment specific conditions, 14 (28 total) for root QTLs found in both treatments, and four for shoot size traits. Using transcriptome analyses, we found gene enrichment in N-related biological processes which may form part of a nitrate treatment developmental response affecting root angle. These findings provide a genetic insight into plant N adaptive responses and targets that could help improve N capture in wheat.

Acknowledgements

This work was supported by the Biotechnology and Biological Sciences Research Council, UK (BB/M001806/1, BB/L026848/1, BB/P026834/1, and BB/M019837/1)(MJB, DMW, and MPP); the Leverhulme Trust, UK (RPG-2016–409) (MJB and DMW); the European Research Council FUTUREROOTS Advanced Investigator Grant, UK (294729) to MG, JAA, DMW, and MJB; and the University of Nottingham Future Food Beacon of Excellence, UK. The authors would like to thank Limagrain UK Ltd. for the use of the S×R DH population and Luzie U. Wingen (John Innes Centre) for providing the R/qtl scripts used in this work.

Declaration of competing interest

The authors declare that they have no conflict of interest.

Appendices associated with this paper are available on <http://www.ChinaAgriSci.com/V2/En/appendix.htm>

References

- Akpınar B A, Kantar M, Budak H. 2015. Root precursors of microRNAs in wild emmer and modern wheats show major differences in response to drought stress. *Functional & Integrative Genomics*, **15**, 587–598.
- Altschul S F, Gish W, Miller W, Myers E W, Lipman D J. 1990. Basic local alignment search tool. *Journal of Molecular Biology*, **215**, 403–410.
- An D, Su J, Liu Q, Zhu Y, Tong Y, Li J, Jing R, Li B, Li Z. 2006. Mapping QTLs for nitrogen uptake in relation to the early growth of wheat (*Triticum aestivum* L.). *Plant and Soil*, **284**, 73–84.
- Anders S, Huber W. 2010. Differential expression analysis for sequence count data. *Genome Biology*, **11**, R106.
- Antoni R, Dietrich D, Bennett M J, Rodriguez P L. 2016. Hydrotropism: Analysis of the root response to a moisture gradient. *Methods in Molecular Biology*, **1398**, 3–9.
- Atkinson J A, Wingen, L U, Griffiths M, Pound M P, Gaju O, Foulkes M J, Le Gouis J, Griffiths S, Bennett M J, King J, Wells D M. 2015. Phenotyping pipeline reveals major seedling root growth QTL in hexaploid wheat. *Journal of Experimental Botany*, **66**, 2283–2292.
- Bai C, Liang Y, Hawkesford M J. 2013. Identification of QTLs associated with seedling root traits and their correlation with plant height in wheat. *Journal of Experimental Botany*, **64**, 1745–1753.
- Beyer S, Daba S, Tyagi P, Bockelman H, Brown-Guedira G, Mohammadi M. 2019. Loci and candidate genes controlling root traits in wheat seedlings — A wheat root GWAS. *Functional & Integrative Genomics*, **19**, 91–107.
- Bolger A M, Lohse M, Usadel B. 2014. Trimmomatic: A flexible trimmer for Illumina sequence data. *Bioinformatics*, **30**, 2114–2120.
- Broman K W, Wu H, Sen Ś, Churchill G A. 2003. R/qtl: QTL mapping in experimental crosses. *Bioinformatics*, **19**, 889–890.
- Churchill G A, Doerge R W. 1994. Empirical threshold values for quantitative trait mapping. *Genetics*, **138**, 963–971.
- Clark R T, Famoso A N, Zhao K, Shaff J E, Craft E J, Bustamante C D, Mccouch S R, Aneshansley D J, Kochian V. 2013. High-throughput two-dimensional root system phenotyping platform facilitates genetic analysis of root growth and development. *Plant, Cell & Environment*, **36**, 454–466.
- Dawson J C, Huggins D R, Jones S S. 2008. Characterizing nitrogen use efficiency in natural and agricultural ecosystems to improve the performance of cereal crops in low-input and organic agricultural systems. *Field Crops Research*, **107**, 89–101.
- Delogu G, Cattivelli L, Pecchioni N, De Falcis D, Maggiore T, Stanca A M. 1998. Uptake and agronomic efficiency of nitrogen in winter barley and winter wheat. *European Journal of Agronomy*, **9**, 11–20.
- Edgar R C. 2004. MUSCLE: Multiple sequence alignment with high accuracy and high throughput. *Nucleic Acids Research*, **32**, 1792–1797.
- El-Gebali S, Mistry J, Bateman A, Eddy S R, Luciani A, Potter S C, Qureshi M, Richardson L J, Salazar G A, Smart A, Sonnhammer E L L, Hirsh L, Paladin L, Piovesan D, Tosatto S C E, Finn R D. 2019. The Pfam protein families database in 2019. *Nucleic Acids Research*, **47**, D427–D432.
- Falconer D S. 1996. *Introduction to Quantitative Genetics*. 4th ed. Longman Group, London.
- Fang Z, Xia K, Yang X, Grottemeyer M S, Meier S, Rentsch D, Xu X, Zhang M. 2013. Altered expression of the PTR/NRT1 homologue OsPTR9 affects nitrogen utilization efficiency, growth and grain yield in rice. *Plant Biotechnology Journal*, **11**, 446–458.

- FAO (Food and Agriculture Organization of United Nations). 2019. *World Fertilizer Trends and Outlook to 2020*. Rome, Italy. [2021-02-21]. <http://www.fao.org/publications/card/en/c/CA6746EN/>
- Gaju O, Allard V, Martre P, Snape J W, Heumez E, LeGouis J, Moreau D, Bogard M, Griffiths S, Orford S, Hubbart S, Foulkes M J. 2011. Identification of traits to improve the nitrogen-use efficiency of wheat genotypes. *Field Crops Research*, **123**, 139–152.
- Gelli M, Duo Y, Konda A R, Zhang C, Holding D, Dweikat I. 2014. Identification of differentially expressed genes between sorghum genotypes with contrasting nitrogen stress tolerance by genome-wide transcriptional profiling. *BMC Genomics*, **15**, 1–16.
- Good A G, Johnson S J, De Pauw M, Carroll R T, Savidov N, Vidmar J, Lu Z, Taylor G, Stroehrer V. 2007. Engineering nitrogen use efficiency with alanine aminotransferase. *Canadian Journal of Botany*, **85**, 252–262.
- Guo Y, Kong F, Xu Y, Zhao Y, Liang X, Wang Y, An D, Li Si. 2012. QTL mapping for seedling traits in wheat grown under varying concentrations of N, P and K nutrients. *Theoretical and Applied Genetics*, **124**, 851–865.
- Habash D Z, Bernard S, Schondelmaier J, Weyen J, Quarrie S A. 2007. The genetics of nitrogen use in hexaploid wheat: N utilisation, development and yield. *Theoretical and Applied Genetics*, **114**, 403–419.
- Haley C S, Knott S A. 1992. A simple regression method for mapping quantitative trait loci in line crosses using flanking markers. *Heredity*, **69**, 315–324.
- Henderson C R. 1975. Best linear unbiased estimation and prediction under a selection model. *Biometrics*, **31**, 423–444.
- Ho C H, Lin S H, Hu H C, Tsay Y F. 2018. CHL1 functions as a nitrate sensor in plants. *Cell*, **138**, 1184–1194.
- Hodge A, Berta G, Doussan C, Merchan F, Crespi M. 2009. Plant root growth, architecture and function. *Plant and Soil*, **321**, 153–187.
- Huang N C, Liu K H, Lo H J, Tsay Y F. 1999. Cloning and functional characterization of an Arabidopsis nitrate transporter gene that encodes a constitutive component of low-affinity uptake. *Plant Cell*, **11**, 1381–1392.
- Husson F, Josse J, Le S, Maintainer J M. 2019. R Package “FactoMineR”: Multivariate exploratory data analysis and data mining. [2019-08-05]. <https://github.com/husson/FactoMineR>
- IWGSC (International Wheat Genome Sequencing Consortium). 2018. Shifting the limits in wheat research and breeding using a fully annotated reference genome. *Science*, **361**, eaar7191.
- Kanno Y, Hanada A, Chiba Y, Ichikawa T, Nakazawa M, Matsui M, Koshiba T, Kamiya Y, Seo M. 2012. Identification of an abscisic acid transporter by functional screening using the receptor complex as a sensor. *Proceedings of the National Academy of Sciences of the United States of America*, **109**, 9653–9658.
- Kant S, Bi Y M, Rothstein S J. 2011. Understanding plant response to nitrogen limitation for the improvement of crop nitrogen use efficiency. *Journal of Experimental Botany*, **62**, 1499–1509.
- Kawahara Y, de la Bastide M, Hamilton J P, Kanamori H, McCombie W R, Ouyang S, Schwartz D C, Tanaka T, Wu J, Zhou S, Childs K L, Davidson R M, Lin H, Quesada-Ocampo L, Vaillancourt B, Sakai H, Lee S S, Kim J, Numa H, Itoh T, et al. 2013. Improvement of the *Oryza sativa* nipponbare reference genome using next generation sequence and optical map data. *Rice*, **6**, 3–10.
- Krogh A, Larsson B, Von Heijne G, Sonnhammer E L L. 2001. Predicting transmembrane protein topology with a hidden Markov model: Application to complete genomes. *Journal of Molecular Biology*, **305**, 567–580.
- Krouk G, Lacombe B, Bielach A, Perrine-Walker F, Malinska K, Mounier E, Hoyerova K, Tillard P, Leon S, Ljung K, Zazimalova E, Benkova E, Nacry P, Gojon A. 2010. Nitrate-regulated auxin transport by NRT1.1 defines a mechanism for nutrient sensing in plants. *Developmental Cell*, **18**, 927–937.
- Kuznetsova A, Brockhoff P B, Christensen R H B. 2017. lmerTest package: Tests in linear mixed effects models. *Journal of Statistical Software*, **82** 1–26.
- Landjeva S, Neumann K, Lohwasser U, Börner A. 2008. Molecular mapping of genomic regions associated with wheat seedling growth under osmotic stress. *Plant Biology*, **52**, 259–266.
- Lark R M, Milne A E, Addiscott T M, Goulding K W T, Webster C P, O’Flaherty S. 2004. Scale- and location-dependent correlation of nitrous oxide emissions with soil properties: An analysis using wavelets. *European Journal of Soil Science*, **55**, 611–627.
- Léran S, Varala K, Boyer J C, Chiurazzi M, Crawford N, Daniel-Vedele F, David L, Dickstein R, Fernandez E, Forde B, Gassmann W, Geiger D, Gojon A, Gong J M, Halkier B A, Harris J M, Hedrich R, Limami A M, Rentsch D, Seo M, et al. 2014. A unified nomenclature of nitrate transporter 1/peptide transporter family members in plants. *Trends in Plant Science*, **19**, 5–9.
- Liu X, Li R, Chang X, Jing R. 2013. Mapping QTLs for seedling root traits in a doubled haploid wheat population under different water regimes. *Euphytica*, **189**, 51–66.
- Lobet G, Pound M P, Diener J, Pradal C, Draye X, Godin C, Javaux M, Leitner D, Meunier F, Nacry P, Pridmore T P, Schnepf A. 2015. Root system markup language: Toward a unified root architecture description language. *Plant Physiology*, **167**, 617–627.
- Miller A J, Fan X, Orsel M, Smith S J, Wells D M. 2007. Nitrate transport and signalling. *Journal of Experimental Botany*, **58**, 2297–2306.
- Mooney S J, Pridmore T P, Helliwell J, Bennett M J. 2012. Developing X-ray computed tomography to non-invasively image 3-D root systems architecture in soil. *Plant and Soil*, **352**, 1–22.
- Oono Y, Kawahara Y, Yazawa T, Kanamori H, Kuramata M, Yamagata H, Hosokawa S, Minami H, Ishikawa S, Wu J,

- Antonio B, Handa H, Itoh T, Matsumoto T. 2013. Diversity in the complexity of phosphate starvation transcriptomes among rice cultivars based on RNA-Seq profiles. *Plant Molecular Biology*, **83**, 523–537.
- Ouellette L A, Reid R W, Blanchard S G, Brouwer C R. 2018. LinkageMapView-rendering high-resolution linkage and QTL maps. *Bioinformatics*, **34**, 306–307.
- Pertea M, Kim D, Pertea G M, Leek J T, Salzberg S L. 2016. RNA-seq experiments with HISAT, StringTie and Ballgown. *Nature Protocols*, **11**, 1650–1667.
- Pound M P, French A P, Atkinson J A, Wells D M, Bennett M J, Pridmore T. 2013. RootNav: Navigating images of complex root architectures. *Plant Physiology*, **162**, 1802–1814.
- Raudvere U, Kolberg L, Kuzmin I, Arak T, Adler P, Peterson H, Vilo J. 2019. g:Profiler: A web server for functional enrichment analysis and conversions of gene lists 2019 update. *Nucleic Acids Research*, **47**, W191–W198.
- Remans T, Nacry P, Pervent M, Filleur S, Diatloff E, Mounier E, Tillard P, Forde B G, Gojon A. 2006. The Arabidopsis NRT1.1 transporter participates in the signaling pathway triggering root colonization of nitrate-rich patches. *Proceedings of the National Academy of Sciences of the United States of America*, **103**, 19206–19211.
- Ren Y, He X, Liu D, Li J, Zhao X, Li B, Tong Y, Zhang A, Li Z. 2012. Major quantitative trait loci for seminal root morphology of wheat seedlings. *Molecular Breeding*, **30**, 139–148.
- Rich S M, Christopher J, Richards R, Watt M. 2020. Root phenotypes of young wheat plants grown in controlled environments show inconsistent correlation with mature root traits in the field. *Journal of Experimental Botany*, **71**, 4751–4762.
- Roselló M, Royo C, Sanchez-Garcia M, Soriano J M. 2019. Genetic dissection of the seminal root system architecture in Mediterranean durum wheat landraces by genome-wide association study. *Agronomy*, **9**, 364.
- Schindelin J, Arganda-Carrera I, Frise E, Kaynig V, Longair M, Pietzsch T, Preibisch S, Rueden C, Saalfeld S, Schmid B, Tinevez J V, White D J, Hartenstein V, Eliceiri K, Tomancak P, Cardona A. 2012. Fiji: An open-source platform for biological-image analysis. *Nature Methods*, **9**, 676–682.
- Stamatakis A. 2014. RAxML version 8: A tool for phylogenetic analysis and post-analysis of large phylogenies. *Bioinformatics*, **30**, 1312–1313.
- Sun J, Guo Y, Zhang G, Gao M, Zhang G, Kong F, Zhao Y, Li S. 2013. QTL mapping for seedling traits under different nitrogen forms in wheat. *Euphytica*, **191**, 317–331.
- Takahashi N, Goto N, Okada K, Takahashi H. 2002. Hydrotropism in abscisic acid, wavy, and gravitropic mutants of *Arabidopsis thaliana*. *Planta*, **216**, 203–211.
- Trachsel S, Kaeppler S M, Brown K M, Lynch J P. 2013. Maize root growth angles become steeper under low N conditions. *Field Crops Research*, **140**, 18–31.
- Wang S, Wong D, Forrest K, Allen A, Chao S, Huang B E, Maccaferri M, Salvi S, Milner S G, Cattivelli L, Mastrangelo A M, Whan A, Stephen S, Barker G, Wieseke R, Plieske J, International Wheat Genome Sequencing Consortium, Lillemo M, Mather D, Appels R. 2014. Characterization of polyploid wheat genomic diversity using a high-density 90 000 single nucleotide polymorphism array. *Plant Biotechnology Journal*, **12**, 787–796.
- Watt M, Moosavi S, Cunningham S C, Kirkegaard J A, Rebetzke G J, Richards R A. 2013. A rapid, controlled-environment seedling root screen for wheat correlates well with rooting depths at vegetative, but not reproductive, stages at two field sites. *Annals of Botany*, **112**, 447–455.
- Wei T, Simko V. 2017. R package ‘corrplot’: Visualization of a CORRELATION Matrix. version 0.84. [2020-07-28]. <https://github.com/taiyun/corrplot>
- Xu C, Zhang H, Sun J, Guo Z, Zou C, Li W X, Xie C, Huang C, Xu R, Liao H, Wang J, Xu X, Wang S, Xu Y. 2018. Genome-wide association study dissects yield components associated with low-phosphorus stress tolerance in maize. *Theoretical and Applied Genetics*, **131**, 1699–1714.
- Yang M, Wang C R, Hassan M A, Wu Y Y, Xia X. 2020. QTL mapping of seedling biomass and root traits under different nitrogen conditions in bread wheat (*Triticum aestivum* L.). *Journal of Integrative Agriculture*, **19**, 2–14.
- Yu G, Smith D K, Zhu H, Guan Y, Lam T T Y. 2017. Ggtree: An R package for visualization and annotation of phylogenetic trees with their covariates and other associated data. *Methods in Ecology and Evolution*, **8**, 28–36.
- Yu P, Eggert K, von Wirén N, Li C, Hochholdinger F. 2015. Cell type-specific gene expression analyses by RNA sequencing reveal local high nitrate-triggered lateral root initiation in shoot-borne roots of maize by modulating auxin-related cell cycle regulation. *Plant Physiology*, **169**, 690–704.
- Zhang H, Cui F, Wang L, Li J, Ding A, Zhao C, Bao Y, Yang Q, Wang H. 2013. Conditional and unconditional QTL mapping of drought-tolerance-related traits of wheat seedling using two related RIL populations. *Journal of Genetics*, **92**, 213–231.
- Zimin A V, Marçais G, Puiu D, Roberts M, Salzberg S L, Yorke J A. 2013. The MaSuRCA genome assembler. *Bioinformatics*, **29**, 2669–2677.
- Zurek P R, Topp C N, Benfey P N. 2015. Quantitative trait locus mapping reveals regions of the maize genome controlling root system architecture. *Plant Physiology*, **167**, 1487–1496.